# PERFORMANCE ANALYSIS OF MILITARY FLYING WING UAV WITH PULSE JET ENGINE

**Vasile PRISACARIU**

"Henri Coandă" Air Force Academy, Brașov, Romania (prisacariu.vasile@afahc.ro)
ORCID: 0000-0003-4370-4756

DOI: 10.19062/1842-9238.2022.20.2.4

***Abstract:*** *The current technological level of data acquisition systems, used on military and civilian unmanned aircraft, allow for diverse kinetic sampling conditions covering large ranges of altitudes and temperature. Thus, there is a need to collect the necessary atmospheric data, in terms of constructive simplicity and reduction of total costs (manufacturing and operation), with the help of unmanned aircraft equipped with PJE (pulse jet engine) and PDE (pulse detonation engine) propulsion systems. The article presents pre-design aspects of a flying wing UAV concept equipped with a PJE engine, which can be mounted on supersonic aircraft.*

***Keywords:*** *flying wing, pulse jet engine, pulse detonation engine, XFLR5*

***Symbols and acronyms***

| | | | |
|---|---|---|---|
| *AR* | *Aspect ratio* | *AoA* | *Angle of attack* |
| *CAD* | *Computer Aided Design* | *CAM* | *Computer Aided Manufacturing* |
| *CFD* | *Computational fluid dynamics* | *ISR* | *Intelligence, surveillance, and reconnaissance* |
| *LLT* | *Lifting line theory* | *MAC* | *Main aerodynamic chord* |
| *PDE* | *Pulse detonation engine* | *PJE* | *Pulse jet engine* |
| *VLM* | *Vortex Lattice Method* | | |
| $c_0$ | *Root chord* | $c_e$ | *Tip chord* |
| $c_l$, | *Lift coefficient* | $c_m$ | *Pitch coefficient* |
| $c_d$, | *Drag coefficient* | | |

## 1. INTRODUCTION

PDEs are propulsion systems, in experimental phases, that use supersonic detonation waves as a combustion mechanism, having a reduced mechanical complexity and high efficiency compared to traditional aerofoil engines, PDE being considered an extension of PJE [5].

Due to the thermodynamic conditions of combustion, it can be an eligible candidate for equipping UAVs for subsonic and supersonic kinetic conditions, under the conditions of a UAV concept optimized for atmospheric data acquisition missions at high altitudes.

PDE can be an eligible technical solution for the propulsion of UAVs with fixed wing in classic concept or tailless (flying wing) in airborne launch conditions. Starting from the Fi 103 (V1) missile, historical and evolutionary milestones have confirmed the usefulness of (military) UAVs, such as: AQM-34 Firebee (Fig. 1.1), Lockheed D-21 (Fig. 1.2), BQM-74), equipped with no rotor engine-PJE engines.

The PDE concept offers a number of advantages, the most relevant being: technological and design simplicity, record theoretical power per volume unit, they are ecological, low impact on the engine and aircraft structure.

However, the concept of PDEs does not offer commercial applications with technological limitations still to be solved, such as: ignition of the detonation wave in a controllable and reliable way, geometric optimization of the detonation tube, cycle repetition frequency, optimization of manufacturing materials, [5]. Along with technological progress, the PDE concept is analysed multidisciplinary by the scientific community, a concept subject to concerns in the field of experimental thermodynamics and CFD analyses, [4].

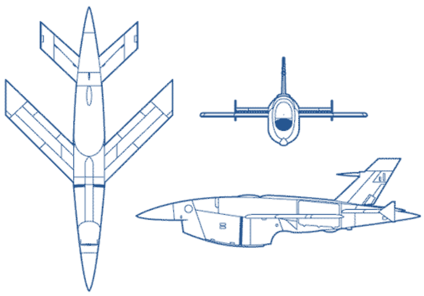

**FIG. 1.1** AQM-34 Firebee, [1]

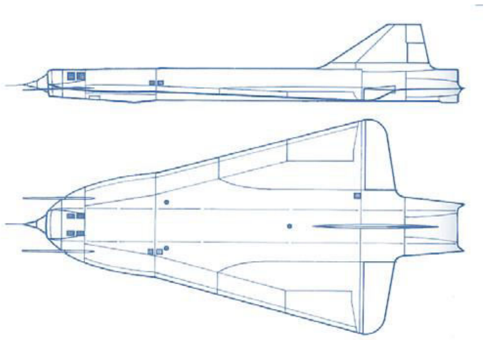

**FIG. 1.2** Lockheed D 21, [2]

According to specialist information [8, 9] a PDE engine was used on modified Scaled Composites-EZ (Fig. 1.3) thus demonstrating the efficiency of using such a propulsion system in terms of fuel consumption versus traction characteristics and of the level of atmospheric pollution. PJE engines are used in UAS and general and sport aviation, [10, 11].

**FIG 1.3** Rutan Long-EZ Borealis cu PDE, [8, 9]

**FIG 1.4** Glider PJE, [10]

## 2.AERODYNAMIC PERFORMANCE EVALUATION TOOLS AND METHODS

### 2.1. XFLR5 software

XFLR5 provides a series of useful modules for geometric parameterization and aerodynamic performance evaluation (2D and 3D) for aircraft without the influence and interference generated by propulsion systems (propellers). For XFLR5 6.55, the modules are as follows: direct foil design (geometric parameterization of aerofoils), Xfoil inverse design (generation of profiles from selected/edited aerofoils), Xdirect analysis (analysis of aerofoil performances), wing and plane design (geometric parameterization) and 3D aerodynamic analysis single geometries/complex geometries).

For 3D aerodynamic analysis the software tool can use a number of methods such as: LLT (lifting line theory), VLM (vortex lattice method) and 3D panels. The results of the analyses are graphic, numerical with possibilities of poor processing and use with other software tools (e.g. CAD/CAM software, Excel), [7, 13].

**2.2. Aerodynamic analysis methods**

*a. The VLM method*

VLM (Vortex Latice Method) is an extension of the LLT (lifting line theory) method, based on the theory of ideal flow (potential flow), used both in the pre-design stages of aircraft (for a quick estimation of global aerodynamic characteristics) and in the field aerospace university and provides a reasonable level of accuracy. Through the initial estimates of the pressure distribution on the wing, the structural design phases of the fixed (wing, wings) and mobile (flaps, ailerons, thruster) bearing surfaces can be initiated, see Fig. 2.1.

VLM models fixed aerofoil surfaces (wing, tailplanes) as a thin web of discrete vortices for the calculation of lift and induced drag without the influence of wing thickness, turbulence, boundary layer and air viscosity. However, the method offers a global approach to the distribution of the pressure coefficient that determines the quantification of the relevant aerodynamic coefficients (and derived quantities) for possible evaluations of the stability/manoeuvrability qualities for the conceptual phase of the aircraft, [17, 18].

The method is described clearly and in detail in a series of specialized references in the field of aerodynamics, the most relevant being: Katz-Plotkin [19], Anderson [20], Bertin-Simth [21] or Drela [22].

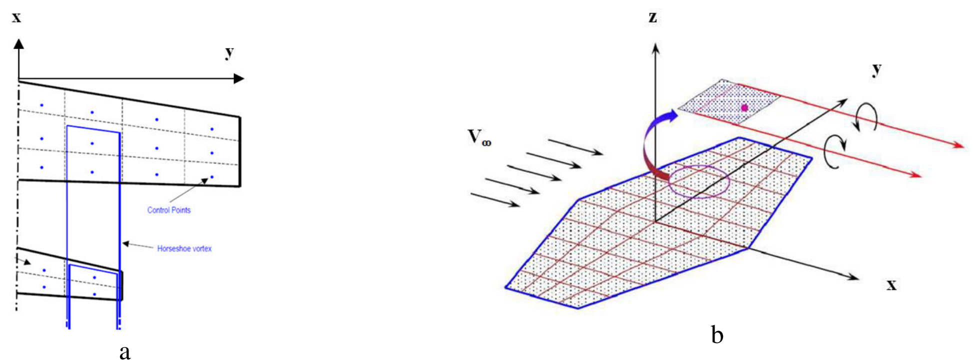


**FIG 2.1** VLM method a.[18], b.[23]

*b. The 3D panel method*

This method analyses the distribution of the pressure coefficient (intrados/extrados) of a bearing surface also considering the thickness of the wing (3D geometry) compared to the VLM which was based only on the curvature line of the wing (2D geometry), see Fig. 2.2.

3D panel models the perturbation existing on the wing surface, initially being an analysis method with singularities (source distributions and vortices) later being a variant of boundary element methods. Currently this method can be used for a solution of the flow potential equation on complex geometries for subsonic or supersonic speeds, the method eliminating the need for a volumetric grid as in the case of finite element methods, [18].

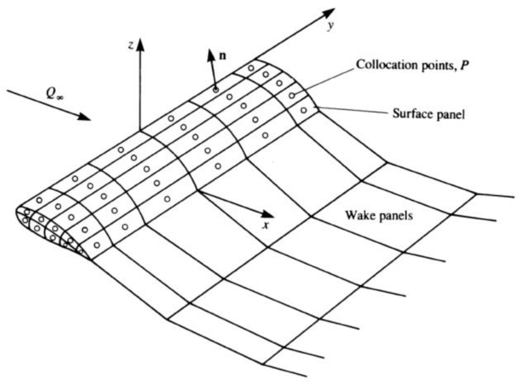


**FIG 2.2** 3D panel method, geometry approximation by panel elements [19]

## 3.CONCEPT FLYING WING UAV-PJE

The UAV-PJE concept is realized with the software tool XFLR5 [6, 7] based on a flying wing geometry (see Fig. 2.1) that can be used in ISR missions, powered by a miniPJE engine, having the characteristics estimated in Table 2.1.

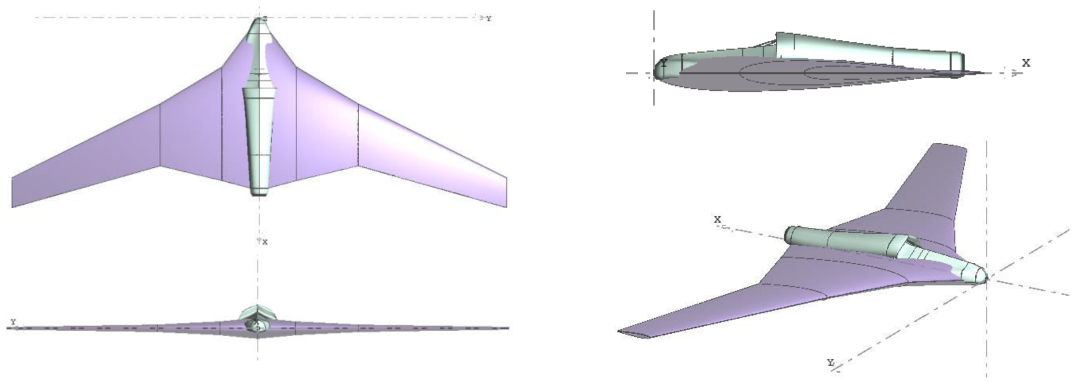

**FIG. 2.1** UAV-PJE/PDE initial proposal concept

*Table 2.1 Initial estimated characteristics for FW UAV-PJE*

| Characteristics | Value | Characteristics | Value |
|---|---|---|---|
| Span / Length | 2 / 1,5 m | MAC | 0,35 m |
| Dihedral / Swept | $5^{o}$ / $26{,}79^{o}$ | Wing load | 8,1 kg/$m^2$ |
| Surface | 0,574 $m^2$ | Total weight/ Payload | 4,65 kg / 1,25 kg |
| Aspect ratio / taper ratio | 6,97 / 0,171 | Propulsion | PJE / pulse-jet |

The estimation of the mass and balance variant is highlighted graphically in Fig. 2.2 and numerically in Table 2.2 and annex 3.

*Table 2.2 FW UAV-PJE weight and balance*

| Element | Value | Element | Value |
|---|---|---|---|
| Frame weight | 2,2 kg | Fuel | 0,5 kg |
| Engine weight | 1,2 kg | Battery | 0,25 kg |
| Electronic equipment weight | 0,5 | Total weight | 4,65 kg |

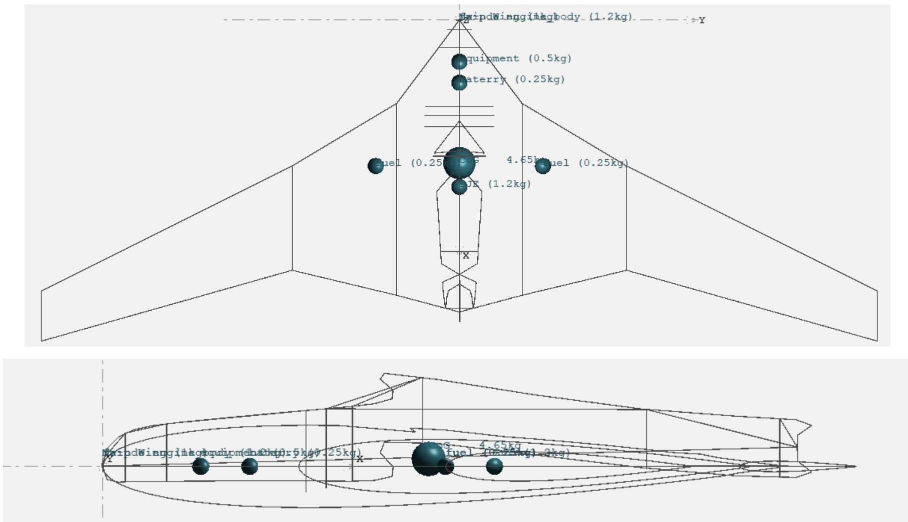

**FIG. 2.2** UAV-PJE weight and balance for initial proposal concept

To make a 3D model, XFLR5 can export *.stl files used for 3D printing with the Cura 15 tool, see Fig. 2.3, [15]. The 3D model can be used to measure aerodynamic parameters in subsonic wind tunnels, [16].

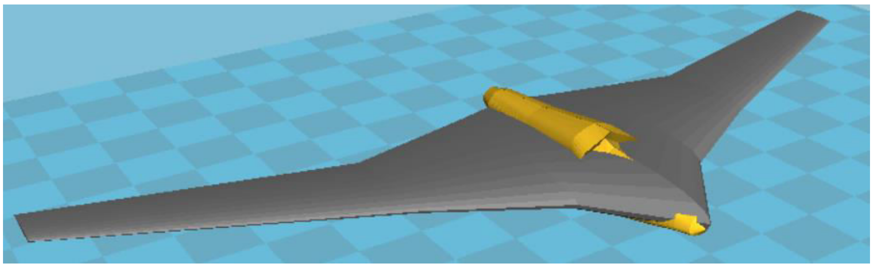

**FIG. 2.3** Model *.stl for 3D print, [15]

## 4.UAV-PJE PERFORMANCES ANALYSIS

### 4.1. Simulation conditions and analysis cases

For optimal parametrisation from the point of view of the useful space of the wing, a high-thickness profile specific to the MH 92 flying wings was chosen for the fitting, and for the extreme section the MH 64 was selected, thus generating a mixed geometric torsion, both designed by Martin Hepperle, see Fig. 3.1, having the characteristics in Table 3.1, [12].

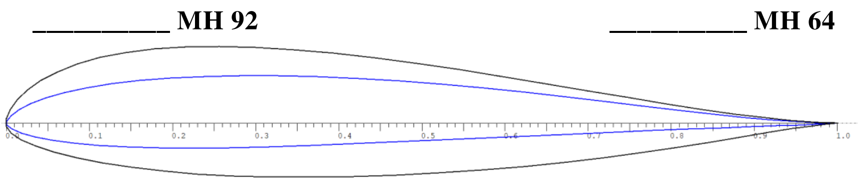


**FIG. 3.1** Aerofoils [13]

*Table 3.1 Aerofoil features*

| MH 92 | | MH 64 | |
|---|---|---|---|
| Max. thickness | 15,50% la 27,5% | Max. thickness | 8,6% la 26,9% |
| Max. curvature | 1,4% la 15% | Max. curvature | 1,4% la 41,8% |

### 4.2. Performance analysis for 2D geometry (XFLR5)

The simulation steps aim at an estimation of the aerodynamic performance of the proposed geometric configuration (see Table 2.1). according to the analysis conditions recorded in Table 3.2.

*Table 3.2 2D analysis conditions*

| Analysis condition | Value | Analysis condition | Value |
|---|---|---|---|
| Chord | 1m | Speed | 15 m/s |
| Nr. Reynolds | 1100000 | Air density | 1,225 kg/m$^3$ |
| Iterations | 100 | Aer viscosity | 1,5 x 10$^{-5}$ m$^2$/s |

The analysed aerofoils provide the variation of comparative values over the range of AoA analysed to observe the aerodynamic behaviour at a minimum theoretical speed (15 m/s).

__________ **MH 92 aerofoil** __________ **MH 64 aerofoil**

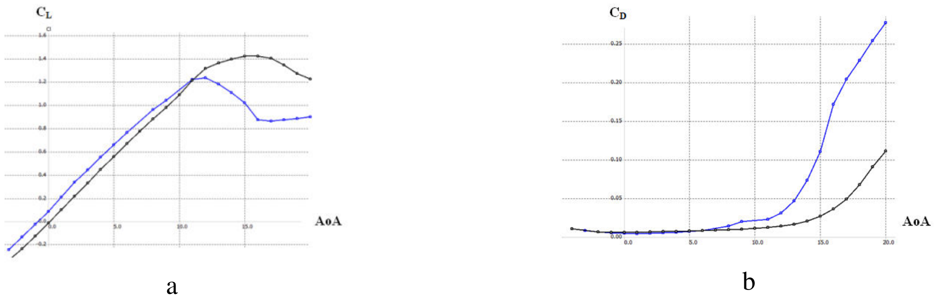


**FIG. 3.2** Airfoil polars, a.$c_l$ vs AoA, b.$c_d$ vs AoA, [13]

Fig. 3.2 and 3.3 show both the polars of the relevant aerodynamic coefficients $c_l$, $c_d$ and $c_m$ as a function of AoA, as well as the gliding rate $c_l/c_d$ vs AoA at the analysed speed (Fig. 3.2c) or the mutual variations of $c_l$ vs $c_d$ (Fig. 3.2.d).

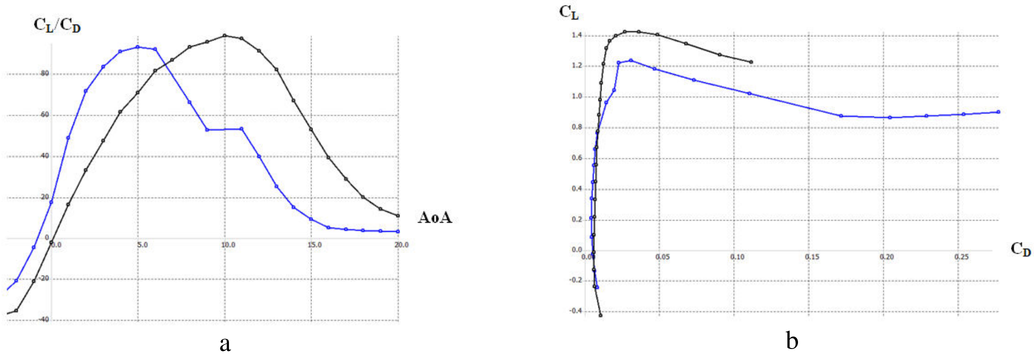


**FIG. 3.3** Aerofoil polars, c. $c_l/c_d$ vs AoA, d.$c_l$ vs $c_d$ [13]

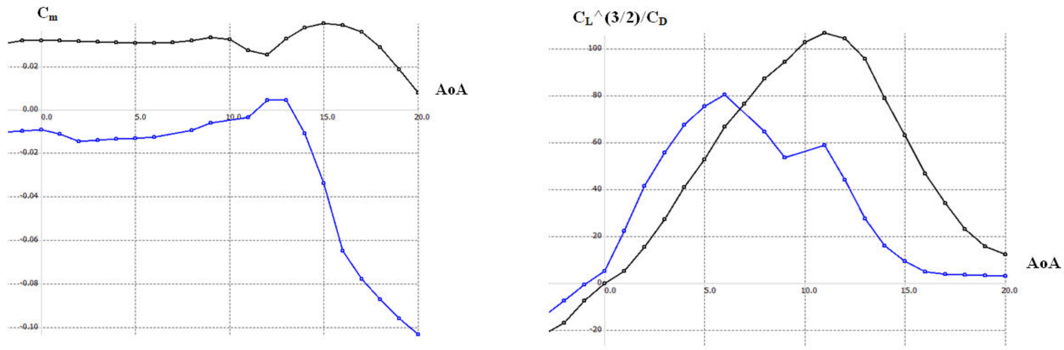


a b

**FIG. 3.4** Aerofoil polars, a.$c_m$ vs AoA, b. $(c_l/c_d)^{3/2}$ vs AoA [13]

The differences in the values of the aerodynamic coefficients for the two analysed aerofoils recommend their use in the span: MH 92 at the embedment and MH 64 at the tip of the wing. The pitching moment differences (Fig. 3.4.a) recommend an optimization of the overall performance through aerodynamic torsion (see also annex 1).

### 4.3. 3D geometry performance analysis

It is focused on a series of aerodynamic analyses for the single flying wing without the presence and influence of the fuselage in the form of aerodynamic interferences, having the atmospheric and kinetic analysis conditions from Table 3.3.

*Table 3.3 3D analysis conditions*

| Analysis condition | Value | Analysis condition | Value |
|---|---|---|---|
| Span | 2 m | Speed | 15 m/s |
| Surface | 0,57 m$^2$ | Boundary conditions | Dirichlet |
| AoA | -15$^o$ ÷ 15$^o$ | AoA precision | 0,01 |
| Method of analysis | VLM/3D panel | Panels VLM / 3D | 494 / 1014 |

The analysed 3D geometry (see also Table 2.1) provides a series of aerodynamic parameter values, highlighted in Fig. 3.5 and 3.6 and Annex 2.

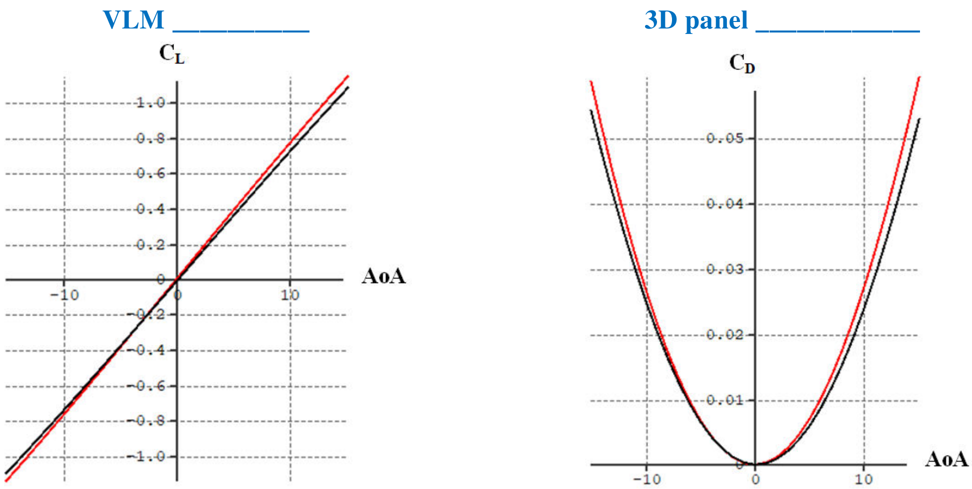


a b

**FIG. 3.5** UAV-PJE flying wing polars, a.Cl-AoA, b.Cd-AoA [13]

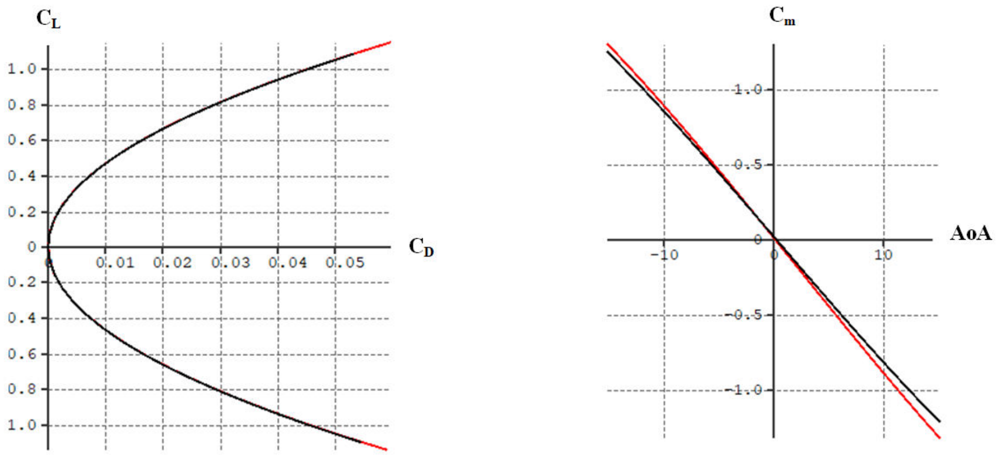


c d

**FIG. 3.6** UAV-PJE flying wing polars, c.$C_l$-$C_d$, d.$C_m$-AoA [13]

According to Fig. 3.5 and 3.6 differences in the values of the aerodynamic coefficients are observed with the increase of AoA due to the consideration of the friction effect in the case of the 3D panel method.

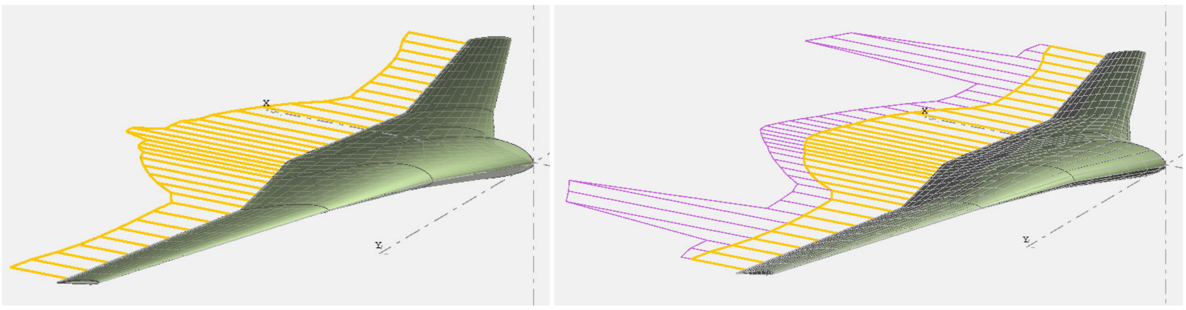

a b

**FIG. 3.7** Drag force (AoA=9$^o$), a.VLM method, b. 3D panel method

In Fig. 3.7, we have the comparative values of the drag for a critical value AoA=9$^o$, and can be observed the trace of the drag generated by the air viscosity. In Fig. 3.8 the values of the pressure coefficient Cp extracted with the two analysis methods: VLM and 2D panel are observed, generated value differences generated by the consideration of air viscosity.

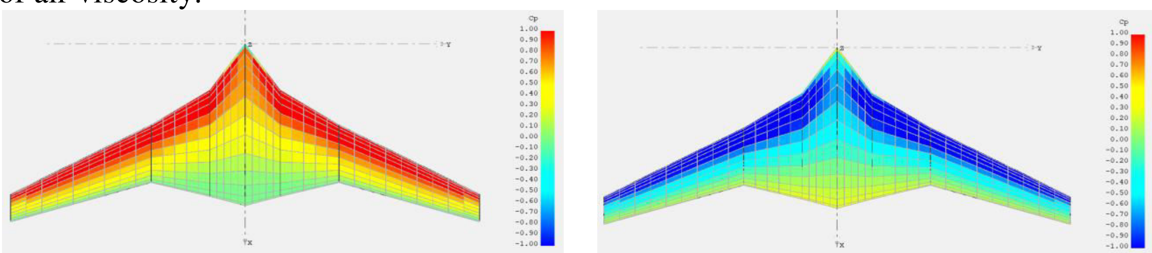

a b

**FIG. 3.8** Pressure coefficient distribution $C_p$ (AoA=9$^o$), a.VLM method, b. 3D panel method

## 5. PROPULSION SYSTEM (PJE) PERFORMANCE ESTIMATE

A mass-optimized PJE for the analysed UAV (maximum weight of 4.65 kg) has the dimensions estimated from Table 5.1, values obtained with Pulse Jet Engine Calculator 1.4 [24]. Figure 5.1. shows a simple PJE geometry with the main dimensions calculated.

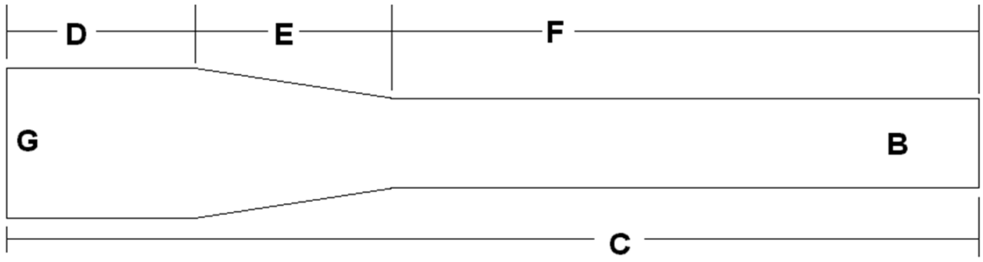


a

b

**FIG. 5.1** Pulse jet engine a.geometry a.[24], b. CAD aspects,[25]

*Table 5.1 PJE structural features and performances estimated*

| Features | Value | Features | Value |
|---|---|---|---|
| Lenght C | 68 cm | Valve head lenght | 10.21 cm |
| Lenght combustor D | 13,62 cm | Exhaust cone E | 13,62 |
| Exhaust pipe F | 40,86 | Detonation freguency | 189-203 Hz |
| Exhaust B | 4,75 cm | Thrust | 5kg/cm |

## CONCLUSIONS

Currently, PJE-powered unmanned aircraft are a mature technology that can offer advantages to users in areas of interest, technology that is also refined with the help of analysis software tools.

The article summarized a pre-design stage of a PJE powered flying wing UAV using freeware tools (XFLR5, PJE calculator).

The current study can be substantiated with the help of CFD tools that can provide high degrees of confidence both in problematic kinetic cases (transonic speeds) and in manoeuvrings flight situations (high angles of attack, high bank angles). In the future, it is considered that the CFD instrumentation will be applied to virtual and real geometric models for a comparative approach to the results and the choice of optimized technical solutions.

## REFERENCES

[1] Freebee UAV, https://www.globalsecurity.org/intell/systems/firebee.htm, accesed in 21.09.2022;

[2] Colville, Jesse & Lewis, Mark & Starkey, Ryan. (2006). *Axisymmetric Inlet Design for Combined-Cycle Engines. Journal of Propulsion and Power* - J PROPUL POWER. 22. 1049-1058. 10.2514/1.18063;

[3] V. Prisacariu, *The history and the evolution of UAVs from the beginning till the 70s*, Journal of Defense Resources Management, vol.8 issue 1(14)/2017, ISSN:2068-9403, eISSN:2247-6466, ISSN-L: 2247-6466, p181-189;

[4] S. Cassady, *Pulse detonation engine*, 2006, available at http://large.stanford.edu/courses/2016/ph240/cassady1/ , accessed on 12.11.2022;
[5] S.L. Deshmukh, *Pulse detonation engine – future of aerospace propulsion*, 2021, available https://dras.in/pulse-detonation-engines-future-of-aerospace-propulsion, accessed on 18.12.2022;
[6] M. Drela, H. Yungren, *Guidelines for XFLR5 v6.03 (Analysis of foils and wings operating at low Reynolds numbers),* 2011, available at http://sourceforge.net/projects/xflr5/files;
[7] V. Prisacariu, *Analysis of UAVs flight characteristics*, vol. 38, nr. 3/2018, p.29-36, Review of the Air Force Academy, ISSN 1842-9238; e-ISSN 2069-4733, DOI: 10.19062/1842-9238.2018.16.3.4;
[8] S.J. Ajitesh, T. Mahant, *Pulse detonation engine - a review*, International Research Journal of Modernization in Engineering Technology and Science, Vol.4, issue 05, 2022, e-ISSN: 2582-5208;
[9] L. Barr, *Puse detonation engine flies into history*, 2008, available at https://www.af.mil/News/Article-Display/Article/123534/pulsed-detonation-engine-flies-into-history, accesed in 18.01.2023;
[10] https://wave-engine.com/technology, accesed in 21.02.2023;
[11] https://www.airtoi.com/pulse.htm, accesed in 14.02.2023;
[12] M. Hepperle, https://www.mh-aerotools.de/airfoils/mh64koo.htm, accesed in 16.02.2022;
[13] XFLR%, https://www.xflr5.tech/xflr5.htm, accesed in 16.02.2022;
[14] M. Hepperle, https://www.mh-aerotools.de/airfoils/mh92koo.htm, 16.02.2022;
[15] Ultimaker, *Cura 13 user manual*, v.10, 41p., available at https://docs.rs-online.com/a10b/0900766b81376d80.pdf;
[16] *Tunel de vânt Sangari SES 115*, disponibil la https://sangari.ro/index.php/ses115, accesat la data de 15.05.2022;
[17] NASA, *Vortex-lattice utilization*. NASA SP-405, NASA-Langley, Washington, 1976;
[18] *XFLR5 Analysis of foils and wings operating at low Reynolds numbers*, Guidelines for QFLR5 v0.03, 2009, available at https://engineering.purdue.edu/~aerodyn/AAE333/FALL10/HOMEWORKS/HW13/XFLR5_v6.01_Beta_Win32%282%29/Release/Guidelines.pdf;
[19] J. Katz and A. Plotkin, *Low-Speed Aerodynamics From Wing Theory to Panel Methods*, McGraw-Hill, Inc., New York, 1991;
[20] J.D. Anderson Jr, *Fundamentals of aerodynamics*, 2nd ed., McGraw-Hill Inc, 1991;
[21] J.J. Bertin, M.L. Smith, *Aerodynamics for Engineers*, 3rd ed., Prentice Hall, New Jersey, 1998;
[22] M. Drela, *Flight Vehicle Aerodynamics, MIT Press*, Cambridge, MA, 2014;
[23] Huang, Wei & Li, Binbin & Liang, Hui & Chen, Xiaobo. (2016). *Dynamic course stability of towing systems using fiber ropes*, Marine Operations Specialty Symposium (MOSS 2016) , ISBN: 978-981-11-0743-6, doi:10.3850/978-981-11-0743-6 MOSS1015;
[24] E. Beck, Eric Beck's Pulsejet Calculator Version 1.4, available at https://www.jetzilla.com/jetZilla.html;
[25] Kovesdi L., *Pulse jet PL-25*, 2014, available at https://grabcad.com/library/pulse-jet-engine-pl-35-

# Anexx 1. 2D data export

xflr5 v6.55

Calculated polar for: MH64 © Martin Hepperle

1 1 Reynolds number fixed          Mach number fixed

xtrf =   1.000 (top)        1.000 (bottom)
Mach =   0.044      Re =      1.100 e 6     Ncrit =   9.000

| alpha | CL | CD | CDp | Cm | Top Xtr | Bot Xtr | Cpmin | Chinge | XCp | | |
|---|---|---|---|---|---|---|---|---|---|---|---|
| -7.000 | -0.6218 | 0.03382 | 0.03139 | -0.0212 | 0.9526 | 0.0090 | -4.1838 | 0.0000 | 0.0000 | 0.0000 | 0.2118 |
| -6.000 | -0.5487 | 0.02674 | 0.02354 | -0.0187 | 0.8810 | 0.0118 | -3.3770 | 0.0000 | 0.0000 | 0.0000 | 0.2123 |
| -5.000 | -0.4446 | 0.02540 | 0.02174 | -0.0170 | 0.8384 | 0.0182 | -2.4238 | 0.0000 | 0.0000 | 0.0000 | 0.2087 |
| -3.000 | -0.2430 | 0.00847 | 0.00268 | -0.0113 | 0.7659 | 0.0118 | -1.9976 | 0.0000 | 0.0000 | 0.0000 | 0.2008 |
| -2.000 | -0.1341 | 0.00647 | 0.00113 | -0.0102 | 0.7311 | 0.2117 | -1.3695 | 0.0000 | 0.0000 | 0.0000 | 0.1710 |
| -1.000 | -0.0250 | 0.00539 | 0.00088 | -0.0098 | 0.6967 | 0.4759 | -0.4855 | 0.0000 | 0.0000 | 0.0000 | -0.1481 |
| 0.000 | 0.0844 | 0.00481 | 0.00072 | -0.0091 | 0.6512 | 0.6780 | -0.4154 | 0.0000 | 0.0000 | 0.0000 | 0.3564 |
| 1.000 | 0.2092 | 0.00429 | 0.00077 | -0.0112 | 0.5831 | 0.9778 | -0.5479 | 0.0000 | 0.0000 | 0.0000 | 0.3017 |
| 2.000 | 0.3369 | 0.00472 | 0.00084 | -0.0147 | 0.4934 | 1.0000 | -0.7241 | 0.0000 | 0.0000 | 0.0000 | 0.2914 |
| 3.000 | 0.4450 | 0.00534 | 0.00111 | -0.0140 | 0.3959 | 1.0000 | -0.9345 | 0.0000 | 0.0000 | 0.0000 | 0.2787 |
| 4.000 | 0.5529 | 0.00609 | 0.00152 | -0.0135 | 0.3038 | 1.0000 | -1.2262 | 0.0000 | 0.0000 | 0.0000 | 0.2710 |
| 5.000 | 0.6600 | 0.00711 | 0.00213 | -0.0130 | 0.2057 | 1.0000 | -2.0487 | 0.0000 | 0.0000 | 0.0000 | 0.2657 |
| 6.000 | 0.7660 | 0.00835 | 0.00301 | -0.0126 | 0.1190 | 1.0000 | -3.1175 | 0.0000 | 0.0000 | 0.0000 | 0.2615 |
| 8.000 | 0.9601 | 0.01457 | 0.00941 | -0.0092 | 0.0083 | 1.0000 | -5.0423 | 0.0000 | 0.0000 | 0.0000 | 0.2525 |
| 9.000 | 1.0400 | 0.02001 | 0.01543 | -0.0058 | 0.0069 | 1.0000 | -6.2572 | 0.0000 | 0.0000 | 0.0000 | 0.2473 |
| 10.000 | 1.1297 | 0.02195 | 0.01763 | -0.0046 | 0.0050 | 1.0000 | -8.2534 | 0.0000 | 0.0000 | 0.0000 | 0.2445 |
| 11.000 | 1.2202 | 0.02312 | 0.01887 | -0.0034 | 0.0032 | 1.0000 | -10.4633 | 0.0000 | 0.0000 | 0.0000 | 0.2417 |
| 12.000 | 1.2263 | 0.03184 | 0.02838 | 0.0048 | 0.0022 | 1.0000 | -10.9410 | 0.0000 | 0.0000 | 0.0000 | 0.2336 |
| 13.000 | 1.1720 | 0.04812 | 0.04547 | 0.0039 | 0.0022 | 1.0000 | -10.7108 | 0.0000 | 0.0000 | 0.0000 | 0.2326 |
| 14.000 | 1.0972 | 0.07533 | 0.07332 | -0.0122 | 0.0022 | 1.0000 | -10.0683 | 0.0000 | 0.0000 | 0.0000 | 0.2454 |
| 15.000 | 1.0107 | 0.11272 | 0.11115 | -0.0350 | 0.0024 | 1.0000 | -8.8762 | 0.0000 | 0.0000 | 0.0000 | 0.2680 |

xflr5 v6.55

Calculated polar for: MH92 © Martin Hepperle

1 1 Reynolds number fixed          Mach number fixed

xtrf =   1.000 (top)        1.000 (bottom)
Mach =   0.044      Re =      1.100 e 6     Ncrit =   9.000

| alpha | CL | CD | CDp | Cm | Top Xtr | Bot Xtr | Cpmin | Chinge | XCp | | |
|---|---|---|---|---|---|---|---|---|---|---|---|
| -14.000 | -0.5713 | 0.15597 | 0.15438 | 0.0374 | 1.0000 | 0.0181 | -1.8024 | 0.0000 | 0.0000 | 0.0000 | 0.2984 |
| -13.000 | -0.5590 | 0.13769 | 0.13613 | 0.0282 | 1.0000 | 0.0181 | -1.9795 | 0.0000 | 0.0000 | 0.0000 | 0.2840 |
| -12.000 | -0.5709 | 0.11241 | 0.11088 | 0.0156 | 1.0000 | 0.0180 | -2.3847 | 0.0000 | 0.0000 | 0.0000 | 0.2617 |
| -11.000 | -0.9953 | 0.03217 | 0.02846 | -0.0083 | 1.0000 | 0.0098 | -6.2514 | 0.0000 | 0.0000 | 0.0000 | 0.2289 |
| -9.000 | -0.9134 | 0.01788 | 0.01236 | 0.0111 | 0.8228 | 0.0068 | -5.4607 | 0.0000 | 0.0000 | 0.0000 | 0.2516 |
| -8.000 | -0.8524 | 0.01328 | 0.00706 | 0.0198 | 0.7689 | 0.0120 | -4.9014 | 0.0000 | 0.0000 | 0.0000 | 0.2636 |
| -7.000 | -0.7477 | 0.01264 | 0.00641 | 0.0213 | 0.7209 | 0.0158 | -3.8884 | 0.0000 | 0.0000 | 0.0000 | 0.2697 |
| -4.000 | -0.4261 | 0.01055 | 0.00391 | 0.0247 | 0.5863 | 0.0197 | -1.8045 | 0.0000 | 0.0000 | 0.0000 | 0.3011 |
| -2.000 | -0.2339 | 0.00663 | 0.00161 | 0.0304 | 0.4939 | 0.5185 | -1.0432 | 0.0000 | 0.0000 | 0.0000 | 0.3741 |
| -1.000 | -0.1267 | 0.00604 | 0.00145 | 0.0317 | 0.4580 | 0.6797 | -0.6171 | 0.0000 | 0.0000 | 0.0000 | 0.4955 |
| 0.000 | -0.0129 | 0.00603 | 0.00146 | 0.0319 | 0.4190 | 0.7463 | -0.7453 | 0.0000 | 0.0000 | 0.0000 | 2.7257 |
| 1.000 | 0.1018 | 0.00620 | 0.00160 | 0.0318 | 0.3821 | 0.7959 | -0.8780 | 0.0000 | 0.0000 | 0.0000 | -0.0723 |
| 2.000 | 0.2170 | 0.00653 | 0.00178 | 0.0315 | 0.3422 | 0.8242 | -1.0323 | 0.0000 | 0.0000 | 0.0000 | 0.0964 |
| 3.000 | 0.3314 | 0.00698 | 0.00207 | 0.0312 | 0.3071 | 0.8461 | -1.1945 | 0.0000 | 0.0000 | 0.0000 | 0.1473 |
| 4.000 | 0.4454 | 0.00726 | 0.00242 | 0.0310 | 0.2901 | 0.8713 | -1.3616 | 0.0000 | 0.0000 | 0.0000 | 0.1714 |
| 5.000 | 0.5575 | 0.00789 | 0.00287 | 0.0307 | 0.2562 | 0.8851 | -1.5517 | 0.0000 | 0.0000 | 0.0000 | 0.1852 |
| 6.000 | 0.6696 | 0.00822 | 0.00326 | 0.0306 | 0.2444 | 0.9051 | -1.7558 | 0.0000 | 0.0000 | 0.0000 | 0.1938 |
| 7.000 | 0.7765 | 0.00896 | 0.00397 | 0.0311 | 0.2153 | 0.9234 | -2.0012 | 0.0000 | 0.0000 | 0.0000 | 0.1985 |
| 8.000 | 0.8819 | 0.00949 | 0.00453 | 0.0319 | 0.2017 | 0.9415 | -2.2928 | 0.0000 | 0.0000 | 0.0000 | 0.2012 |
| 9.000 | 0.9820 | 0.01031 | 0.00531 | 0.0333 | 0.1772 | 0.9609 | -2.5862 | 0.0000 | 0.0000 | 0.0000 | 0.2023 |
| 10.000 | 1.0914 | 0.01110 | 0.00621 | 0.0324 | 0.1650 | 0.9789 | -2.9549 | 0.0000 | 0.0000 | 0.0000 | 0.2051 |
| 11.000 | 1.2154 | 0.01256 | 0.00753 | 0.0274 | 0.1323 | 0.9910 | -3.3795 | 0.0000 | 0.0000 | 0.0000 | 0.2109 |
| 12.000 | 1.3158 | 0.01452 | 0.00931 | 0.0257 | 0.1010 | 1.0000 | -3.8266 | 0.0000 | 0.0000 | 0.0000 | 0.2122 |
| 13.000 | 1.3636 | 0.01672 | 0.01147 | 0.0330 | 0.0810 | 1.0000 | -4.2314 | 0.0000 | 0.0000 | 0.0000 | 0.2058 |
| 14.000 | 1.3933 | 0.02100 | 0.01579 | 0.0380 | 0.0616 | 1.0000 | -4.7089 | 0.0000 | 0.0000 | 0.0000 | 0.2007 |
| 15.000 | 1.4186 | 0.02707 | 0.02198 | 0.0397 | 0.0526 | 1.0000 | -5.2094 | 0.0000 | 0.0000 | 0.0000 | 0.1977 |

# Anexx 2. 3D data export

```
xflr5 v6.55

Plane name :        fw-pde engine
Polar name :        T1-15.0 m/s-VLM1
Freestream speed :  15.000 m/s
```

| alpha | Beta | CL | CDi | CDv | CD | CY | Cl | Cm | Cn | Cni | QInf | XCP |
|---|---|---|---|---|---|---|---|---|---|---|---|---|
| -15.000 | 0.000 | -1.063660 | 0.051984 | 0.000000 | 0.051984 | -0.000000 | -0.000000 | 1.205421 | -0.000000 | -0.000000 | 15.0000 | 0.4302 |
| -14.000 | 0.000 | -0.994501 | 0.045562 | 0.000000 | 0.045562 | -0.000000 | 0.000000 | 1.130646 | 0.000000 | 0.000000 | 15.0000 | 0.4296 |
| -13.000 | 0.000 | -0.924699 | 0.039496 | 0.000000 | 0.039496 | -0.000000 | 0.000000 | 1.054463 | -0.000000 | -0.000000 | 15.0000 | 0.4290 |
| -12.000 | 0.000 | -0.854296 | 0.033807 | 0.000000 | 0.033807 | -0.000000 | 0.000000 | 0.976965 | -0.000000 | -0.000000 | 15.0000 | 0.4285 |
| -11.000 | 0.000 | -0.783334 | 0.028511 | 0.000000 | 0.028511 | -0.000000 | -0.000000 | 0.898246 | 0.000000 | 0.000000 | 15.0000 | 0.4281 |
| -10.000 | 0.000 | -0.711856 | 0.023627 | 0.000000 | 0.023627 | -0.000000 | -0.000000 | 0.818402 | -0.000000 | -0.000000 | 15.0000 | 0.4278 |
| -9.000 | 0.000 | -0.639907 | 0.019169 | 0.000000 | 0.019169 | -0.000000 | 0.000000 | 0.737531 | -0.000000 | -0.000000 | 15.0000 | 0.4276 |
| -8.000 | 0.000 | -0.567531 | 0.015152 | 0.000000 | 0.015152 | -0.000000 | 0.000000 | 0.655730 | 0.000000 | 0.000000 | 15.0000 | 0.4275 |
| -7.000 | 0.000 | -0.494773 | 0.011587 | 0.000000 | 0.011587 | -0.000000 | 0.000000 | 0.573100 | -0.000000 | -0.000000 | 15.0000 | 0.4275 |
| -6.000 | 0.000 | -0.421681 | 0.008487 | 0.000000 | 0.008487 | -0.000000 | 0.000000 | 0.489742 | 0.000000 | 0.000000 | 15.0000 | 0.4277 |
| -5.000 | 0.000 | -0.348301 | 0.005862 | 0.000000 | 0.005862 | -0.000000 | 0.000000 | 0.405756 | -0.000000 | -0.000000 | 15.0000 | 0.4283 |
| -4.000 | 0.000 | -0.274682 | 0.003719 | 0.000000 | 0.003719 | -0.000000 | 0.000000 | 0.321245 | -0.000000 | -0.000000 | 15.0000 | 0.4293 |
| -3.000 | 0.000 | -0.200870 | 0.002066 | 0.000000 | 0.002066 | -0.000000 | 0.000000 | 0.236312 | -0.000000 | -0.000000 | 15.0000 | 0.4314 |
| -2.000 | 0.000 | -0.126914 | 0.000909 | 0.000000 | 0.000909 | -0.000000 | 0.000000 | 0.151061 | -0.000000 | -0.000000 | 15.0000 | 0.4360 |
| -1.000 | 0.000 | -0.052863 | 0.000251 | 0.000000 | 0.000251 | 0.000000 | 0.000000 | 0.065596 | -0.000000 | -0.000000 | 15.0000 | 0.4543 |
| 0.000 | 0.000 | 0.021234 | 0.000095 | 0.000000 | 0.000095 | 0.000000 | 0.000000 | -0.019980 | 0.000000 | 0.000000 | 15.0000 | 0.3445 |
| 1.000 | 0.000 | 0.095329 | 0.000442 | 0.000000 | 0.000442 | 0.000000 | 0.000000 | -0.105563 | 0.000000 | 0.000000 | 15.0000 | 0.4054 |
| 2.000 | 0.000 | 0.169373 | 0.001291 | 0.000000 | 0.001291 | -0.000000 | 0.000000 | -0.191047 | 0.000000 | 0.000000 | 15.0000 | 0.4131 |
| 3.000 | 0.000 | 0.243316 | 0.002640 | 0.000000 | 0.002640 | 0.000000 | 0.000000 | -0.276329 | 0.000000 | 0.000000 | 15.0000 | 0.4162 |
| 4.000 | 0.000 | 0.317111 | 0.004486 | 0.000000 | 0.004486 | -0.000000 | 0.000000 | -0.361304 | 0.000000 | 0.000000 | 15.0000 | 0.4179 |
| 5.000 | 0.000 | 0.390708 | 0.006823 | 0.000000 | 0.006823 | -0.000000 | 0.000000 | -0.445870 | 0.000000 | 0.000000 | 15.0000 | 0.4191 |
| 6.000 | 0.000 | 0.464060 | 0.009644 | 0.000000 | 0.009644 | -0.000000 | 0.000000 | -0.529924 | 0.000000 | 0.000000 | 15.0000 | 0.4200 |
| 7.000 | 0.000 | 0.537119 | 0.012943 | 0.000000 | 0.012943 | -0.000000 | 0.000000 | -0.613362 | 0.000000 | 0.000000 | 15.0000 | 0.4208 |
| 8.000 | 0.000 | 0.609838 | 0.016708 | 0.000000 | 0.016708 | -0.000000 | 0.000000 | -0.696083 | 0.000000 | 0.000000 | 15.0000 | 0.4216 |
| 9.000 | 0.000 | 0.682170 | 0.020929 | 0.000000 | 0.020929 | -0.000000 | 0.000000 | -0.777987 | 0.000000 | 0.000000 | 15.0000 | 0.4223 |
| 10.000 | 0.000 | 0.754070 | 0.025593 | 0.000000 | 0.025593 | -0.000000 | 0.000000 | -0.858974 | 0.000000 | 0.000000 | 15.0000 | 0.4229 |
| 11.000 | 0.000 | 0.825492 | 0.030688 | 0.000000 | 0.030688 | -0.000000 | 0.000000 | -0.938944 | 0.000000 | 0.000000 | 15.0000 | 0.4236 |
| 12.000 | 0.000 | 0.896392 | 0.036197 | 0.000000 | 0.036197 | -0.000000 | 0.000000 | -1.017801 | 0.000000 | 0.000000 | 15.0000 | 0.4244 |
| 13.000 | 0.000 | 0.966727 | 0.042104 | 0.000000 | 0.042104 | -0.000000 | 0.000000 | -1.095449 | 0.000000 | 0.000000 | 15.0000 | 0.4251 |
| 14.000 | 0.000 | 1.036454 | 0.048391 | 0.000000 | 0.048391 | -0.000000 | 0.000000 | -1.171792 | 0.000000 | 0.000000 | 15.0000 | 0.4259 |
| 15.000 | 0.000 | 1.105531 | 0.055040 | 0.000000 | 0.055040 | -0.000000 | 0.000000 | -1.246739 | 0.000000 | 0.000000 | 15.0000 | 0.4267 |

```
xflr5 v6.55

Plane name :        fw-pde engine
Polar name :        T1-15.0 m/s-Panel
Freestream speed :  15.000 m/s
```

| alpha | Beta | CL | CDi | CDv | CD | CY | Cl | Cm | Cn | Cni | QInf | XCP |
|---|---|---|---|---|---|---|---|---|---|---|---|---|
| -15.000 | 0.000 | -1.086837 | 0.054767 | 0.095650 | 0.150418 | 0.000000 | 0.000000 | 1.271639 | -0.000000 | -0.000000 | 15.0000 | 0.4273 |
| -14.000 | 0.000 | -1.015381 | 0.047916 | 0.095650 | 0.143567 | 0.000000 | 0.000000 | 1.193181 | -0.000000 | -0.000000 | 15.0000 | 0.4282 |
| -13.000 | 0.000 | -0.943261 | 0.041455 | 0.084788 | 0.126243 | 0.000000 | 0.000000 | 1.111920 | -0.000000 | -0.000000 | 15.0000 | 0.4291 |
| -12.000 | 0.000 | -0.870520 | 0.035403 | 0.074675 | 0.110078 | 0.000000 | 0.000000 | 1.029252 | -0.000000 | -0.000000 | 15.0000 | 0.4300 |
| -11.000 | 0.000 | -0.797202 | 0.029779 | 0.065312 | 0.095092 | 0.000000 | 0.000000 | 0.945320 | -0.000000 | -0.000000 | 15.0000 | 0.4311 |
| -10.000 | 0.000 | -0.723354 | 0.024601 | 0.056547 | 0.081148 | 0.000000 | 0.000000 | 0.860237 | -0.000000 | -0.000000 | 15.0000 | 0.4322 |
| -9.000 | 0.000 | -0.649022 | 0.019885 | 0.047991 | 0.067876 | 0.000000 | 0.000000 | 0.774069 | -0.000000 | -0.000000 | 15.0000 | 0.4334 |
| -8.000 | 0.000 | -0.574254 | 0.015645 | 0.030269 | 0.045914 | 0.000000 | 0.000000 | 0.685807 | -0.000000 | -0.000000 | 15.0000 | 0.4348 |
| -7.000 | 0.000 | -0.499098 | 0.011894 | 0.021361 | 0.033255 | 0.000000 | 0.000000 | 0.597887 | 0.000000 | -0.000000 | 15.0000 | 0.4364 |
| -6.000 | 0.000 | -0.423602 | 0.008645 | 0.017839 | 0.026484 | 0.000000 | 0.000000 | 0.509918 | 0.000000 | -0.000000 | 15.0000 | 0.4385 |
| -5.000 | 0.000 | -0.347818 | 0.005906 | 0.014921 | 0.020827 | 0.000000 | 0.000000 | 0.421373 | 0.000000 | -0.000000 | 15.0000 | 0.4412 |
| -4.000 | 0.000 | -0.271794 | 0.003687 | 0.010524 | 0.014211 | 0.000000 | 0.000000 | 0.332126 | 0.000000 | -0.000000 | 15.0000 | 0.4452 |
| -3.000 | 0.000 | -0.195582 | 0.001995 | 0.007342 | 0.009337 | -0.000000 | -0.000000 | 0.242582 | 0.000000 | -0.000000 | 15.0000 | 0.4520 |
| -2.000 | 0.000 | -0.119232 | 0.000834 | 0.006408 | 0.007242 | -0.000000 | -0.000000 | 0.152820 | 0.000000 | -0.000000 | 15.0000 | 0.4668 |
| -1.000 | 0.000 | -0.042797 | 0.000209 | 0.005932 | 0.006141 | -0.000000 | -0.000000 | 0.062753 | -0.000000 | -0.000000 | 15.0000 | 0.5330 |
| 0.000 | 0.000 | 0.033674 | 0.000121 | 0.005667 | 0.005789 | -0.000000 | -0.000000 | -0.027537 | -0.000000 | 0.000000 | 15.0000 | 0.3003 |
| 1.000 | 0.000 | 0.110128 | 0.000572 | 0.005493 | 0.006065 | 0.000000 | -0.000000 | -0.117954 | -0.000000 | 0.000000 | 15.0000 | 0.3913 |
| 2.000 | 0.000 | 0.186514 | 0.001560 | 0.005486 | 0.007046 | 0.000000 | -0.000000 | -0.208396 | -0.000000 | -0.000000 | 15.0000 | 0.4080 |
| 3.000 | 0.000 | 0.262781 | 0.003081 | 0.005715 | 0.008796 | 0.000000 | -0.000000 | -0.298768 | -0.000000 | -0.000000 | 15.0000 | 0.4152 |
| 4.000 | 0.000 | 0.338877 | 0.005132 | 0.006061 | 0.011193 | 0.000000 | -0.000000 | -0.388967 | -0.000000 | -0.000000 | 15.0000 | 0.4192 |
| 5.000 | 0.000 | 0.414752 | 0.007706 | 0.006467 | 0.014174 | 0.000000 | -0.000000 | -0.478883 | -0.000000 | -0.000000 | 15.0000 | 0.4219 |
| 6.000 | 0.000 | 0.490356 | 0.010797 | 0.006964 | 0.017761 | 0.000000 | -0.000000 | -0.568416 | -0.000000 | -0.000000 | 15.0000 | 0.4239 |
| 7.000 | 0.000 | 0.565637 | 0.014393 | 0.007542 | 0.021936 | 0.000000 | -0.000000 | -0.657462 | -0.000000 | -0.000000 | 15.0000 | 0.4254 |
| 8.000 | 0.000 | 0.640548 | 0.018486 | 0.008539 | 0.027025 | 0.000000 | -0.000000 | -0.745984 | -0.000000 | -0.000000 | 15.0000 | 0.4265 |
| 9.000 | 0.000 | 0.715038 | 0.023062 | 0.009905 | 0.032966 | 0.000000 | -0.000000 | -0.833892 | -0.000000 | -0.000000 | 15.0000 | 0.4275 |
| 10.000 | 0.000 | 0.789061 | 0.028107 | 0.024201 | 0.052308 | 0.000000 | -0.000000 | -0.924345 | -0.000000 | -0.000000 | 15.0000 | 0.4283 |
| 11.000 | 0.000 | 0.862569 | 0.033606 | 0.047003 | 0.080609 | 0.000000 | -0.000000 | -1.016548 | -0.000000 | -0.000000 | 15.0000 | 0.4290 |
| 12.000 | 0.000 | 0.935516 | 0.039544 | 0.051560 | 0.091104 | 0.000000 | -0.000000 | -1.103289 | 0.000000 | -0.000000 | 15.0000 | 0.4296 |
| 13.000 | 0.000 | 1.007857 | 0.045900 | 0.055672 | 0.101572 | 0.000000 | -0.000000 | -1.188889 | 0.000000 | -0.000000 | 15.0000 | 0.4301 |
| 14.000 | 0.000 | 1.079547 | 0.052657 | 0.061927 | 0.114584 | 0.000000 | -0.000000 | -1.274412 | 0.000000 | -0.000000 | 15.0000 | 0.4305 |
| 15.000 | 0.000 | 1.150543 | 0.059794 | 0.064219 | 0.124013 | 0.000000 | -0.000000 | -1.357188 | 0.000000 | -0.000000 | 15.0000 | 0.4309 |

# Anexx 3. Mass and balance data export

*fw-pde engine1.mass - Notepad

File Edit Format View Help

```
#-------------------------------------------------
#
#    fw-pde engine
#
#  Dimensional unit and parameter data.
#  Mass & Inertia breakdown.
#-------------------------------------------------
#
Lunit =      0.0010 m
Munit =      1.0000 kg
Tunit = 1.0 s
#-------------------------
#  Gravity and density to be used as default values in trim setup (saves runtime typing).
#  Must be in the unit names given above (i.e. m,kg,s).
g   = 9.81
rho = 1.225
#-------------------------
#  Ixx... are item's inertias about item's own CG.
#
#  x,y,z system here must be exactly the same one used in the .avl input file
#     (same orientation, same origin location, same length units)
#
#     mass        x         y         z        Ixx       Iyy        Izz        Ixy        Ixz        Iyz
         1      403  -7.15e-15        0      0.103    0.0201      0.124          0          0          0 ! Main Wing
       1.2      335         0      29.4   0.000232    0.0405     0.0402          0    0.00102          0 ! Body's inertia
      0.25      350      -200         0      0.000     0.000      0.000 ! fuel
      0.25      350       200         0      0.000     0.000      0.000 ! fuel
       1.2      400         0         0      0.000     0.000      0.000 ! PJE
       0.5      100         0         0      0.000     0.000      0.000 ! equipment
      0.25      150         0         0      0.000     0.000      0.000 ! baterry
#-------------------------
```